

Jet Physics at the Tevatron*

LEE SAWYER

Louisiana Tech University
Ruston, LA 71272

ON BEHALF OF THE CDF AND DØ COLLABORATIONS

The DØ and CDF experiments at Fermi National Accelerator Laboratory's Tevatron collider have each amassed a significant amount of jet events, leading to new results that test the predictions of perturbative Quantum Chromodynamics. Several recent jet physics results are presented, along with a discussion of the prospects for other tests in the coming years.

PACS numbers: 13.87.Ce,12.38.Qk

1. Introduction

The Fermi National Accelerator Laboratory's upgraded Tevatron collider began operation in April, 2001, with two experiments that had also undergone extensive upgrades. In the run period since the collider operations began, known as Run II, each of the experiments has recorded roughly 400 pb^{-1} of data, about four times as much data as was collected during Run I of the Tevatron in 1992 to 1995. By the summer of 2005, when a series of small detector upgrades and accelerator improvements will take place, the experiments are expected to record around 1 fb^{-1} of data.

Both the CDF[1] and the DØ[2] experiments are general purpose collider detectors that are designed to measure a wide variety of processes at the Tevatron. Both have central tracking systems that include silicon-strip based microvertex detectors, calorimetry that covers a wide range in pseudorapidity η , and muon detectors down to small angles.

* Presented at the International Symposium on Multiparticle Dynamics, Sonoma State University, CA, 28 July 2004

The upgrade to the Tevatron did not result in improved luminosity alone. The collider is now running at a proton-antiproton center of mass energy of 1.96 TeV, compared to 1.8 TeV in Run I. While this may seem like a small increase in energy, it does create a significant increase in physics reach in the steeply falling cross-sections characteristic of high p_T physics. The cross-section for jets with $p_T = 400$ GeV/c is a factor of two higher in Run II, and at 600 GeV/c (roughly the highest p_T jets seen in Run I) the cross-section is six times higher [3].

While many important jet measurements were made in Run I, there remains a rich menu of studies that can be done at the Tevatron. The higher center of mass energy and increased luminosity allow better probes of very high p_T jets, which in turn allows probes of the proton structure at high x . Tests of perturbative Quantum Chromodynamics (pQCD) with improved statistics are possible, as well as searches for new high-mass states that decay into pairs of jets. Since jet production predominates all other high p_T physics process at the Tevatron, a detailed understanding of jets is also necessary as a background study to other physics measurements and searches.

This note will discuss some of the basic ideas involved in jet physics at the Tevatron, and present a summary of recent Run II jet results. Due to space limitations few of the plots shown at the conference will be included; the reader is referred to the CDF[4] and DØ[5] public results webpages for plots and the most recent approved results.

2. Jet Definitions

The quarks and gluons produced in high energy hadron collisions are not directly observed, rather we infer their presence from collimated jets of particles observed in our detectors. One of the primary tasks in jet physics is to relate the jet observables to their parton-level counterparts. The first step in doing this is to carefully define exactly what is meant by a jet. A more complete description of jet algorithms at the Tevatron is given in Bernard Andriu's talk in these proceedings. Briefly, there are two classes of jet algorithms that are being used at the Tevatron: cone algorithms and the k_T algorithm.

Cone algorithms are based on the association of energy deposition in the experiment's calorimeter to a cone of fixed radius in $\eta - \phi$ space. In DØ, the Run II cone algorithm is implemented with radius $R_{\text{cone}} = 0.7$. Any "particle" (Monte Carlo generator particle, calorimeter tower, reconstructed track, etc.) can in principle be used, though for the analyses discussed in this note only calorimeter towers are included. A cone of $dR = \sqrt{(\Delta\eta)^2 + (\Delta\phi)^2} < R_{\text{cone}}$ is formed around initial "seed" towers

having $p_T > p_T^{\min} = 8$ GeV/c. Particle 4-vectors are added to the cone to produce a proto-jet. A new cone is formed around the proto-jet, and the process iterated until a stable solution found. At this point the cone axis is identified as the jet axis. Proto-jets are removed if they have $p_T < p_T^{\min}$. Jets are merged if more than the overlap fraction $f (=50\%)$ of p_T^{jet} is contained in the overlap region; otherwise the jets are split. Finally the midpoints between pairs of jets are used as additional seeds; this final restoring infrared safety to the jet-finding process.

In CDF, the JETCLU algorithm is used, again with $R_{\text{cone}} = 0.7$ for most of the jet physics analyses. JETCLU differs from DØ's RunII cone algorithm primarily in that: 1) JETCLU adds E_T s of clusters in the cone, according to the so-called Snowmass prescription[6]; and 2) JETCLU does not use midpoints between pairs of jets as seeds.

Besides the cone algorithm, both experiments are developing the so-called k_T algorithm for jet analyses. The k_T algorithm is not a fixed cone algorithm, but rather uses the relative momenta of particles, merged by pairs. For each pair (i,j) of particles, the quantity $D_{\min} = \min(p_T^2(i), p_T^2(j))\Delta R_{ij}/D$ is formed, where $D = \text{Jet Size parameter}$. All particles above threshold are included and the process is infrared safe.

Finally, the jet energy scale typically must be well-understood, particularly if the jet measurements are to be corrected back to the hadron or parton level. Factors impacting the jet energy scale include energy offset (*i.e.* energy not from the hard scattering process), detector response, out-of-cone showering, and resolution. Electromagnetic energy scale determined from $Z \rightarrow ee$ is used to find the hadronic response using p_T -balance in $\gamma + \text{jets}$, along with linearity corrections from calorimeter calibration. Energy scale uncertainties often are the largest systematic errors in jet measurements.

3. Inclusive Jet Cross-Sections

Both CDF and DØ have reported inclusive jet cross sections for Run II. CDF has measured the inclusive jet cross section with the JETCLU cone algorithm and the k_T algorithm. Results for the cone algorithm are shown in Fig. 1a. As suggested in the previous section, this measurement extends the reach of the inclusive cross-section measurement for CDF by 150 GeV. The ratio of the Run I to Run II cross-section is shown in Fig. 2. (Note that the Run I/Run II comparison plot does not take into account luminosity errors.)

The k_T algorithm measurement, shown in Fig. 1b, includes jets in the rapidity region of $0.1 < |y| < 0.7$ have $p_T > 72$ GeV/c. CDF repeats the measurement for various values of the algorithm parameter D . The results diverge from next-to-leading order (NLO) QCD predictions (obtained from

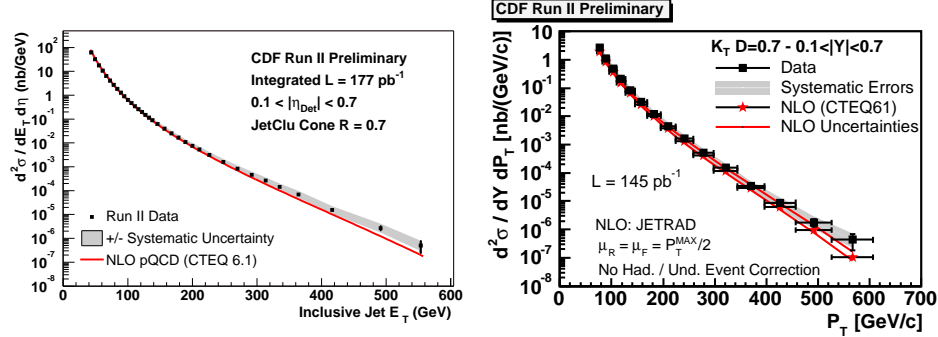


Fig. 1. (a)The CDF inclusive jet cross-section. (b)The CDF inclusive k_T jet cross-section, with comparisons to NLO JETRAD predictions

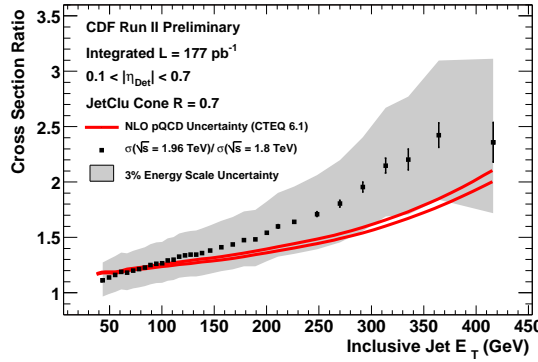


Fig. 2. The ratio of the inclusive jet cross-section at $\sqrt{s} = 1.8$ and 1.96 TeV, compared with NLO pQCD.

JETRAD[7])as D gets large, presumably due to soft gluon contributions.

$D\emptyset$ measures the inclusive jet cross section, using its Run II cone algorithm, three rapidity bins: $|y| < 0.5, 1.5 < |y| < 2.0$, and $2.0 < |y| < 2.4$. As shown in Fig. 3 there is good agreement between the data and NLO corrections obtained from JETRAD. In each plot the CTEQ6M[8] parton distribution function (PDF) is used; note that there is increased uncertainty due to the PDF in the forward region.

4. Dijets

While the inclusive jet cross-section measurements show that the two experiments have all the necessary tools (luminosity, acceptance, trigger, detector systematics) in place to study jet physics, it is the dijet final state

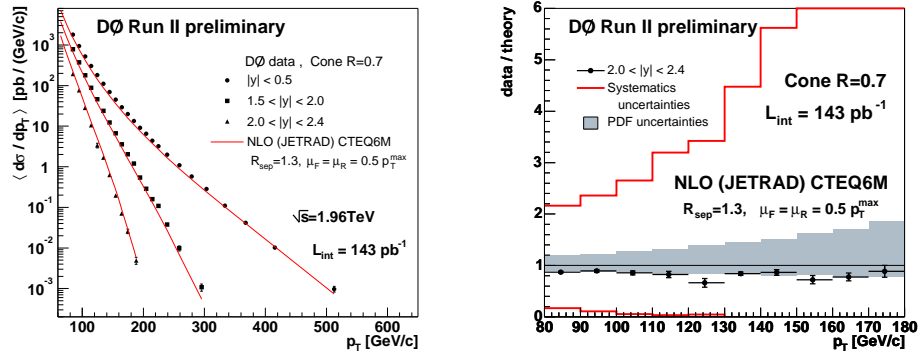


Fig. 3. (a) The DØ inclusive jet cross-section, measured in three rapidity regions. (b) The ratio of data/theory.

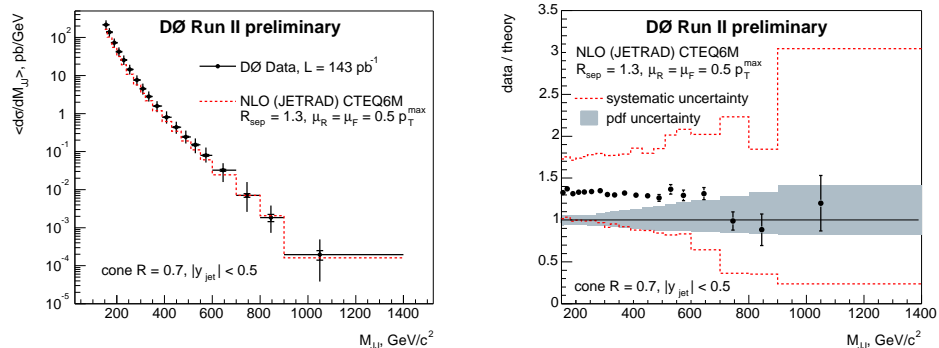


Fig. 4. (a) The DØ dijet cross-section, measured in the central rapidity bin. (b) The ratio of data/theory for the DØ dijet cross-section and NLO prediction from JETRAD.

that provides a channel for searching for new mass resonances, and forms the background to numerous other studies. DØ has measured the dijet cross-section in same three rapidity bins ($0 < |y| < 0.7, 1.5 < |y| < 2.0$, and $2.0 < |y| < 2.4$) as the inclusive cross-section; the resulting spectrum of $d\sigma/dM_{jj}$ for the central rapidity region is shown in Fig. 4a. Figure 4b shows the comparison between data and NLO predictions for the central rapidity bin.

The separation in ϕ of the two leading jets in an event is sensitive to final state radiation. At leading order, there are two partons in the final state giving rise to the jets, and $\Delta\phi = \pi$. At higher order, a hard third jet

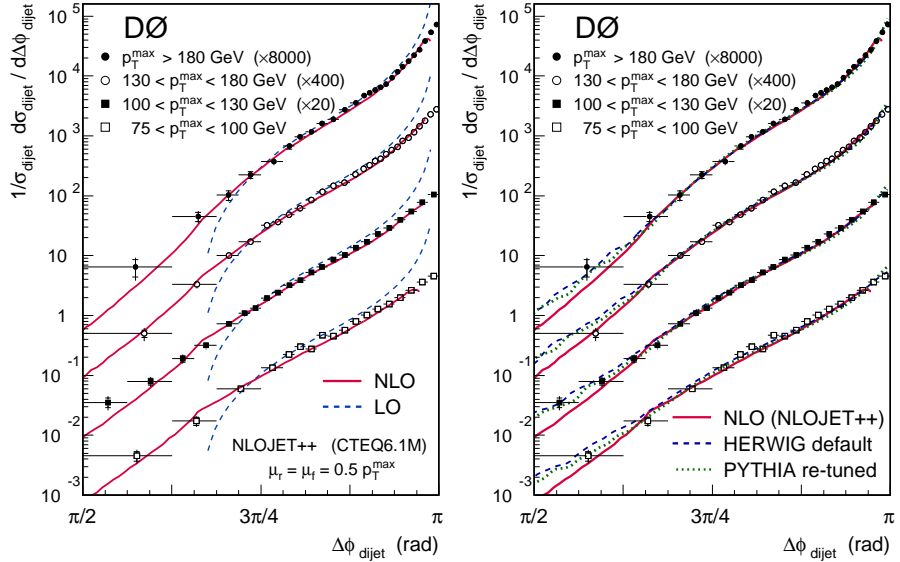


Fig. 5. (a) The DØ $d\phi$ distribution, compared LO and NLO pQCD predictions. (b) The same distribution, compared to three Monte Carlo generators.

($p_{\perp} > 0$) leads to $\Delta\phi < \pi$. Measuring the dijet $\Delta\phi$ spectrum tests $O(\alpha_s)$ QCD predictions.

DØ measures the opening angle between the leading and next-to-leading jet in the central inclusive dijet sample. The advantage of this technique is that there is no need to explicitly measure third or greater jet. The result is shown in Fig. 5, with the data in ranges of the leading jet p_T , and each range normalized to the first bin of the inclusive cross-section. As expected the harder jet events have a spectrum more sharply peaked toward $\Delta\phi = \pi$.

In order to understand the expected contribution from LO and NLO contributions, comparisons are made to fixed-order perturbative QCD (Fig. 5a). The leading order prediction (dashed blue curve) diverges at $\Delta\phi = \pi$ due to the lack of soft processes; while no phase-space remains for $\Delta\phi < 2\pi/3$ (only three partons in the event). The next-to-leading order (solid red curve) provides a good description over the whole range, except in extreme $\Delta\phi$ regions. For comparison, the curves in Fig. 5b show the expected $d\phi$ distributions from the HERWIG[9] and PYTHIA[10] generators (better results from PYTHIA are obtained when the parameter PARP(67), which controls gluon radiation, is tuned to the data).

5. Jet Shapes

CDF has made detailed studies of jet shapes, using the fraction of a jet E_T within a subcone. Defining the energy flow $\Psi = E_T(r)/E_T(R)$, where r and R are the subcone and jet cone radii respectively, CDF measures the energy flow variable in jets reconstructed with the Mid-Point algorithm (similar to the DØ Run II cone algorithm) and corrected back to the hadron level. This measurement is sensitive to multiple gluon emission from the primary parton, as well as being sensitive to underlying event. Plots of $1 - \Psi(r = 0.3)$ vs the p_T of the jet were shown during the conference, as well as comparison plots on the left Monte Carlo generator expectations (from PYTHIA) for gluon- and quark-initiated jets. For further details concerning this measurement and its relation to the underlying event, see Rick Fields's paper in these proceedings.

6. Conclusions

A rich range of QCD topics is to be pursued in Run II of the Tevatron. First results from both the CDF and DØ experiments show generally good agreement with theory for cross-sections. More detailed comparisons to theory are needed for details of event and jet shapes.

In the coming years, both experiments will be able to explore high p_T and M_{jj} regions over a wide range of rapidities. This will allow test high- x gluon contributions, as well as the search for evidence of new physics.

I wish to thank both collaborations, in particular the CDF QCD convenors Rick Fields and Mario Martinez and the DØ QCD convenors Markus Wobisch and Christophe Royon, for their assistance in compiling the results presented in this paper. Any errors are strictly my own.

REFERENCES

- [1] T. Affolder, *et al.*, FERMILAB-Pub-96/390-E.
- [2] DØ Collaboration, F. Last, Nucl. Instr. & Methods A **123**, 456 (2004).
- [3] Gerald C. Blazey, *et al.*, "Run II Jet Physics", from "QCD and Weak Boson Physics in RunII", Fermilab-Pub-00/297; ed. U. Baur, R.K. Ellis, and D. Zeppenfeld.
- [4] http://www-cdf.fnal.gov/physics/new/qcd/qcd03_blessed_run2.html
- [5] <http://www-d0.fnal.gov/Run2Physics/WWW/results/qcd.htm>
- [6] J.E. Huth *et al.* in *Proceedings of Research Directions For The Decade: Snowmass 1990*, July, 1990, ed. E.L. Berger (World Scientific, 1992) p. 134.
- [7] W.T. Giele, E.Q.N. Glover, and D.A. Kosower, Phys. Rev. Lett. 73, 2019 (1994).

- [8] J. Pumplin *et al.*, W.K. Tung, JHEP 07, 12 (2002).
- [9] G. Corcella *et al.*, JHEP 0101, 010 (2001).
- [10] G. Marchesini *et al.*, Comp. Phys. Comm. 67, 465 (1992)